Three kinematical methods to identify local Galactic structures[1]

R. Cubarsi[1], S. Alcobé[1], S. Vidojević[2,3,4], S. Ninković[4,5]

[1]Dept. Matemàtica Aplicada IV, Universitat Politècnica de Catalunya, E08034-Barcelona, Catalonia, Spain. [2]Faculty of Mathematics, University of Belgrade, Studentski trg 16, 11000 Beograd, Serbia. [3]Observatoire de Paris, Section de Meudon, 5 Place Jules Janssen, 92195 Meudon, France. [4] Institute Isaac Newton of Chile, Yugoslavia Branch. [5] Astronomical Observatory, Volgina 7, 11060 Beograd 38, Serbia.

Abstract

Method one: by combining a sampling parameter related to an isolating integral of the stellar motion, an optimisation of the mixture approach, and a maximisation of the partition entropy for the constituent populations of the stellar sample.

Method two: by segregating into different kinematical components in terms of the stellar orbital parameters.

Method three: by approaching a maximum entropy velocity distribution to samples selected in terms of stellar eccentricity layers.

Working samples: HIPPARCOS and Geneva-Copenhagen survey catalog.

Results: kinematical characterisation of large-scale structures, such as thin disc, thick disc and halo, and identification of small-scale structures, such as moving groups in the solar neighbourhood.

Consequences: confirmation of the Titius-Bode-like law for radial velocity dispersions and explanation of the apparent vertex deviation of the disc from the swinging of two major kinematic groups around the LSR, by predicting a continuously changing orientation of the disc pseudo ellipsoid.

Method I: MEMPHIS algorithm

A sampling parameter P is defined to introduce a hierarchy into the sample (Alcobé & Cubarsi 2005 and Cubarsi et al. 2010), so that a set of nested subsamples is recursively drawn from the total sample. Some properties, which are associated with isolating integrals of the star motion, such as the absolute values of the velocity component perpendicular to the Galactic plane, $P = |W|$, of the rotational velocity, $P = |V|$, or of the total velocity $P = |(U, V, W)|$, are used as sampling parameters to discriminate between populations. A bimodal pattern of two Gaussian distributions is recursively applied to identify different kinematic behaviours within each subsample. In each case, the optimal sampling parameter provides the least *informative* subsample associated with the more representative mixture parameters, as well as the least error in the mixture approach.
For samples drawn from the HIPPARCOS catalogue (ESA 1997) and the Geneva-Copenhagen survey (GCS) of the Solar neighbourhood (Nordtröm et al. 2004), the best segregation of thin and thick discs is obtained by using the sampling parameter $P = |(U, V, W)|$, while the halo is detached from the total disc from the sampling parameter $P = |W|$.

Sample	#S	Pop.	P	σ_U	σ_V	σ_W	U	V	W	ε [°]
HIP	12,516	t 91.5%	$\|(U,V,W)\|$ =230	28.2 ± 0.2	16.9 ± 0.2	12.5 ± 0.1	−11.2 ± 0.3	−14.7 ± 0.2	−7.1 ± 0.1	13 ± 1
	1,003	T 7.3%		69.3 ± 1.3	37.9 ± 0.9	42.9 ± 0.9	−7.1 ± 2.2	−60.8 ± 1.2	−9.7 ± 1.4	4 ± 2
	159	H 1.2%	$\|W\|$ =180	179.6 ± 7.8	89.0 ± 6.3	90.8 ± 6.0	−0.61 ± 14.2	−234.9 ± 7.0	−10.8 ± 7.2	−6 ± 3
GCS	12,415	t 93.8%	$\|(U,V,W)\|$ =230	29.7 ± 0.2	17.8 ± 0.2	13.9 ± 0.1	−10.4 ± 0.3	−15.2 ± 0.2	−7.1 ± 0.1	11 ± 1
	763	T 5.7%		65.7 ± 1.5	36.7 ± 1.1	41.5 ± 0.9	−3.4 ± 2.4	−59.3 ± 1.3	−7.1 ± 1.5	5 ± 2
	62	H 0.5%	$\|W\|$ =170	178.6 ± 12.2	113.7 ± 15.0	110.5 ± 14.2	1.6 ± 22.7	−230.8 ± 14.4	−16.4 ± 14.0	−5 ± 10

Table 1: Optimal mixture parameters for the HIPPARCOS (HIP) and GCS samples. The displayed quantities are: size of the optimal sample, sampling parameter, segregated population (t=thin disc, T=thick disc, H=halo) and mixture proportion, velocity dispersions, mean velocities (both in km s^{-1}), and vertex deviation.

Method II: Galactocentric orbits

The orbital parameters are used to classify stars into Galactic subsystems such as the thin disc, the thick disc, and the halo (Vidojević & Ninković 2008, 2009; Cubarsi et al. 2010). For the GCS catalogue, we assume that any star crossing the boundary of 70 kpc adopted in the model of the Galaxy is a halo star. There are 13 such stars in the sample, of which 5 have angular momentum that differs from that of the Galactic rotation. Also, 26 other sample stars with a Galactocentric V component of opposite sign to that of the Galactic rotation are classified as halo stars. Stars of the Galactic disc are expected to move around the Galactic centre in nearly planar orbits so their *vertical eccentricities* should not be significant. For this reason, 25 stars in the sample with $e_v > 0.4$ are classified as halo stars. In the case of nearly planar orbits, stars of the disc are

[1]DYNAMICS AND EVOLUTION OF DISC GALAXIES, 27th Annual Pushchino Conference (May 31 - June 04, 2010). Sternberg Astronomical Institute (Moscow State University) and Pushchino Radio Astronomy Observatory, Moscow, Russia.

not expected to have a very high interval of R so a limit to the *planar eccentricity* should also exist. So 10 sample stars with $e_p > 0.8$ are classified halo stars. There is one sample star that, despite belonging to the halo according to any criterion given above, is assigned to the halo because its highest Z amplitude takes place almost in the middle of the interval in R. Therefore, we finally identify 75 (about 0.5%) halo stars.

Sample	#S	Pop.	σ_U	σ_V	σ_W	U	V	W	ε [°]
GCS	12,566	t 95.0%	30.2 ± 0.4	19.0 ± 0.3	13.5 ± 0.2	-9.6 ± 0.6	-16.1 ± 0.4	-7.1 ± 0.3	10 ± 1
	599	T 4.5%	$67.8^{+4.1}_{-3.6}$	$40.9^{+2.5}_{-2.2}$	$46.2^{+2.8}_{-2.5}$	-16.4 ± 5.5	-52.4 ± 3.3	-7.5 ± 3.7	1 ± 2
	13,165	D 99.5%	32.9 ± 0.4	21.9 ± 0.3	16.5 ± 0.2	-9.9 ± 0.6	-17.4 ± 0.4	-7.1 ± 0.3	10 ± 1
	75	H 0.5%	165^{+32}_{-23}	125^{+24}_{-17}	110^{+21}_{-15}	-6.9 ± 2.1	-201 ± 24	-14.4 ± 3.3	-9 ± 7

Table 2: Segregation of populations for GCS sample from the Galactic orbits of the stars.

The remaining stars belong to the Galactic disc. The variations in the shape and size of Galactocentric orbits for stars of the Galactic disc are correlated with their eccentricities, and for sufficiently high values of both e_p and e_v, the sides of the orbital trapezia become curvilinear. We identified an approximate border where curving of the sides of orbital trapezia begins. We present this border as a broken line in the e_v versus e_p plot for the disc stars. The equations of the straight lines containing the segments are

$$\begin{aligned} e_p \in [0, 0.2]: &\quad e_v = -0.25\, e_p + 0.15, \\ e_p \in [0.2, 0.5]: &\quad e_v = -0.33\, e_p + 0.17. \end{aligned} \tag{1}$$

The vertex occurs at (0.2, 0.1). The points lying inside this broken line, 12,566 (95%), represent the stars of the thin disc, those lying outside it, 599 (4.5%), the thick-disc ones. The elements of the velocity ellipsoid, the mean heliocentric velocity components, dispersions, and the vertex deviation with their uncertainties for the halo, thick disc and thin disc are given in Table 2. In the case of the mean values and dispersions, the uncertainties correspond to the 95% confidence intervals, whereas the uncertainty in the vertex deviation is determined following the formula for error propagation.

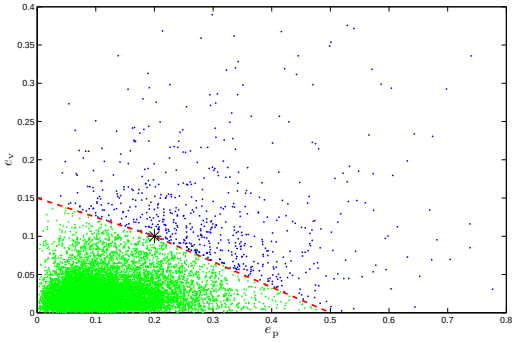

Figure 1: Vertical eccentricity versus planar eccentricity for total disc stars. The broken line (red) separates stars of the thin disc (green) from those of the thick disc (blue).

Titius-Bode-like law (TBLL)

This empirical law (Alcobé & Cubarsi 2005) may be related with the average epicycle energy $E_R \sim \sigma_U^2$ of the stars representative of the disk heating process. For each population, the radial velocity dispersion continuously increases with the sampling parameter $P = |(U, V, W)|$, up to reach some steady values, which are collected by the TBLL. Now, by adding the halo component, we may certainly certify this relationship, and associate the discrete local stellar populations with the radial dispersions expressed by the equation

$$\sigma_U(n) = 6.6 \left(\frac{4}{3}\right)^{3n+2}; \quad n = 0, 1, 2, 3. \tag{2}$$

n	σ_U-TBLL	σ_U-MEMPHIS	stellar pop.
0	6.6	-	spherical pop. at birth
1	12	12	early-type stars
2	28	28	thin disk
3	66	65	thick disk
4	156	156	halo

Method III: Maximum entropy approach

If an extended set of moments is available, this method provides a linear algorithm leading to a fast and suitable estimation of the velocity distribution (Cubarsi 2010). It can be used to model multimodal distributions that cannot be described through Gaussian mixtures. The maximum entropy function has the form

$$f(\mathbf{V}) = e^{\mathcal{P}(\mathbf{V})}, \tag{3}$$

where $\mathcal{P}(\mathbf{V})$ is a power series of the velocity components containing as many terms as the number of moment constraints. The boundary conditions, which are usually assumed for the solutions of the stellar hydrodynamic equations, along with an integral property involving the velocity moments (Cubarsi 2007), lead to a Gramian system of equations to determine the polynomial coefficients of the phase density function.

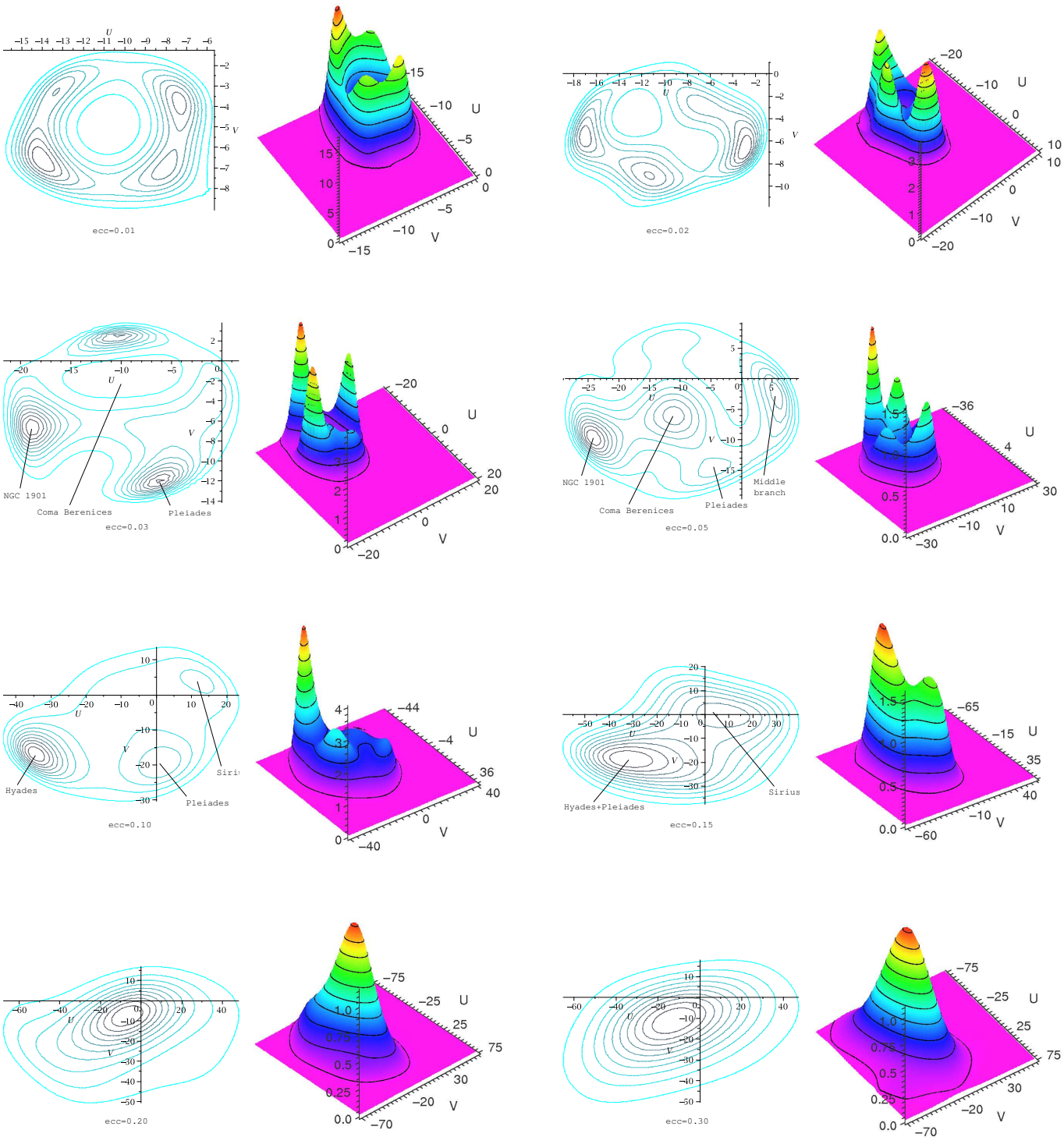

Figure 2: Series of contour plots and distributions on the *UV* plane for GCS subsamples selected from $|z_{max}| < 0.5$ kpc and eccentricities up to 0.01, 0.02, 0.03, 0.05, 0.1, 0.15, 0.2 and 0.3. The origin is at the Solar velocity.

To describe the small-scale disc structure, several truncated distributions have been analysed in terms of metallicity, colour, maximum distance to the Galactic plane, and eccentricity. In particular, the eccentricity, which is directly related to the isolating integrals of the star motion, is more discriminating than the absolute velocity for selecting subsamples. A representative thin disc, containing 90% of the whole sample, is selected from maximum eccentricity 0.3 and $|z_{\max}| \leq 0.5$ kpc. Its central moments are similar to the ones obtained for the thin disc of Tables 1 and 2. Within the thin disc, the eccentricity behaves as an excellent sampling parameter that distinguishes between different eccentricity layers allowing the subjacent structures of Figure 2 to be visualised.

Orientation of the disc velocity pseudo-ellipsoid

For stars with a similar period of oscillation around the LSR in the radial direction (under the epicyclic approximation), several simulations allow us to confirm that a two-peaked distribution of radial velocities, such as for eccentricity 0.01, is due to a lognormal distribution of the eccentricities. For a mixture of stars with different periods and a lognormal distribution of the velocity amplitude of the stellar orbits, the bimodal shape is maintained. However, if the number of stars with nearly vanishing amplitude increases, then the radial velocity distribution becomes unimodal, similar to the total thin disc sample with $e = 0.3$. The bimodal behaviour of the central disc, associated with the previous major subsystems, may then be explained from two different phenomena. On one hand, a perturbation similar to a pressure wave, acting in part along the radial direction, induces an oscillation of the radial velocity around the LSR, with heliocentric velocity (-9.72, -11.45, -6.65) km s^{-1}, obtained from a sample with eccentricities $e \leq 0.15$. On the other hand, both kinematical major groups, which actually are placed at the solar position, are in opposite oscillation states. In addition both groups have a difference of about 20 km s^{-1} in rotation mean velocity, so that one group of stars actually surpasses the other group. Therefore, the apparent vertex deviation of the thin disc may stem from the swinging of those major kinematic groups. A scenario of a continuously changing orientation of the disc pseudo ellipsoid is then possible.

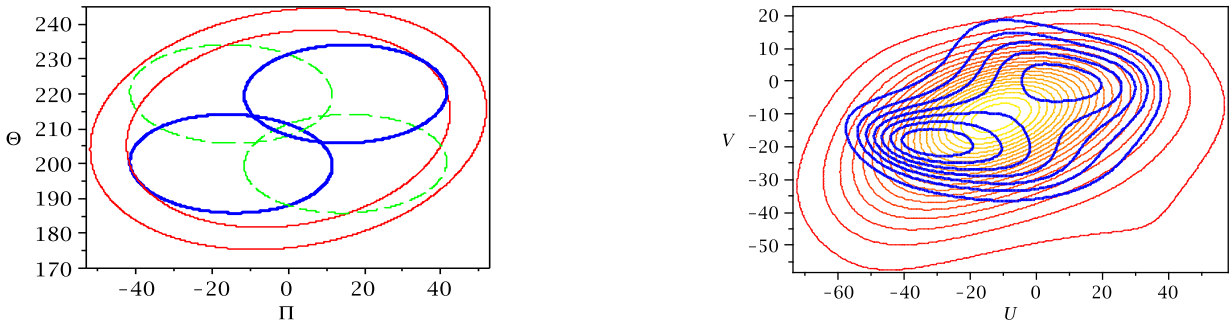

Figure 3: (Left) Velocity ellipsoids depicted from the sample with eccentricities $e \leq 0.15$, in blue. They are centred in Galactocentric velocities $\Pi_0 = 15, \Theta_0 = 220$, and $\Pi_0 = -15, \Theta_0 = 200$, with the LSR placed in the middle of them. In red, the thin disc isocontours, from the sample with eccentricities $e \leq 0.3$, have positive vertex deviation and are generated from the inner structure. The green dashed partial ellipsoids represent a situation with the opposite radial motions. (Right) Contour plots in the UV plane (heliocentric velocities) for the samples with maximum eccentricity $e = 0.15$ (blue) and $e = 0.3$ (red).

References

Alcobé S., Cubarsi R. 2005, A&A, 442, 929
Cubarsi R. 2007, MNRAS 207, 380
Cubarsi R., Alcobé S., Vidojević S., Ninković S. 2010, A&A, 510, A102
Cubarsi R. 2010, A&A, 510, A103
ESA 1997, The Hipparcos Catalogue. ESA SP-1200
Nordström B., Mayor M., Andersen J., Holmberg J., Pont F., Jørgensen B.R., Olsen E.H., Udry S., Mowlavi N. 2004, A&A, 418, 989
Vidojević S., Ninković S. 2008, SerAJ, 177, 39
Vidojević S., Ninković S. 2009, AN, 330, 46